Ordered phases and temperature behaviour of CH_3S self-assembled monolayers on Au(111)

2007 J. Phys.: Condens. Matter 19 305019

(http://iopscience.iop.org/0953-8984/19/30/305019)

IOP PUBLISHING JOURNAL OF PHYSICS: CONDENSED MATTER

J. Phys.: Condens. Matter **19** (2007) 305019 (9pp) doi:10.1088/0953-8984/19/30/305019

Ordered phases and temperature behaviour of CH_3S self-assembled monolayers on Au(111)

Davide Cavanna[1], Gianangelo Bracco[1,4], Valentina De Renzi[2,3], Valdis Corradini[3], Roberto Biagi[2,3] and Umberto del Pennino[2,3]

[1] CNR-INFM and CNR-IMEM, Dipartimento di Fisica dell'Università di Genova, Via Dodecaneso 33, 16146 Genova, Italy
[2] Dipartimento di Fisica, Università di Modena e Reggio Emilia, V. Campi 213/a, 41100, Modena, Italy
[3] CNR-INFM Centre for nanoStructures and bioSystem at Surfaces, V. Campi 213/a, 41100, Modena, Italy

E-mail: bracco@fisica.unige.it

Received 5 February 2007, in final form 7 May 2007
Published 13 July 2007
Online at stacks.iop.org/JPhysCM/19/305019

Abstract

We present the results of an experimental characterization of the ordered phases of CH_3S chemisorbed on Au(111) and of their temperature dependence. The CH_3S self-assembled monolayer has been grown by dosing dimethyl disulfide (DMDS) in ultrahigh vacuum at different substrate temperatures between 200 and 320 K and has been characterized by means of low energy He atom scattering (HAS) with time of flight detection and low energy electron diffraction (LEED) in a temperature range between 150 and 320 K. Upon following an appropriate dosing–annealing procedure, two ordered coexisting phases, i.e. a (3×4) and a $(\sqrt{3} \times \sqrt{3})$ periodicity, have been observed using HAS, in agreement with previous findings. Moreover, a new protocol consisting of a single-step dosing of DMDS at higher pressures (10^{-5} mbar range) has been found to produce both coexisting phases without any need of the annealing step. The temperature behaviour of the ordered phases has been studied using LEED, showing that a first-order phase transition occurs at $\sim$320 K.

1. Introduction

Self-assembled monolayers (SAMs) of thiol-functionalized molecules have been intensively studied because they have proved to be promising materials in many applied fields such as sensor fabrication [1] and biorelated applications [2], in controlling corrosion [3], in lubrication [4], in nanotechnology [5], and for nonlinear optics [6]. Among the SAMs, alkanethiols ($CH_3(CH_2)_{n-1}SH$ or C_n) on Au(111) are one of the best studied systems [7].

[4] Author to whom any correspondence should be addressed.

Porter *et al* observed a hexagonal $(\sqrt{3} \times \sqrt{3})$R30° lattice structure for chains with $n = 2, 4$–17 using both atomic force microscopy and scanning tunnelling microscopy [8, 9] and assigned the threefold hollow site as the preferred adsorption site. In addition to the $(\sqrt{3} \times \sqrt{3})$ hexagonal lattice, a $(3 \times 2\sqrt{3})$ superlattice was also observed by means of x-ray diffraction [10, 11], He atom scattering (HAS) [12–14] and scanning probe techniques [15, 16] for alkanethiols with $n > 8$. In other studies, concentrated on shorter chains ($n < 6$) and employing microscopy techniques, several striped phases have been reported. Dishner *et al* [17] reported in addition to a $(3 \times 2\sqrt{3})$ structure a $(2\sqrt{3} \times \sqrt{3})$ striped phase for methanethiol SAMs.

The results of studies on the deposition of dimethyl disulfide $(CH_3S)_2$ (DMDS) have shown that the molecule undergoes a dissociative adsorption on the Au(111) surface [18–21]. The observed structures obtained adsorbing symmetric dialkyldisulfides or alkanethiols are indistinguishable from each other. In a previous He scattering study on the deposition of DMDS on Au(111) [22], the observed structure of a film, deposited at 200 K and briefly annealed to 330 K, was consistent with a $(\sqrt{3} \times \sqrt{3})$ periodicity. Because some not well resolved peaks were also present, the authors used a procedure with a further dosing and overnight annealing at 290 K to improve the diffraction pattern. This optimized deposition procedure led to a film whose diffraction pattern was interpreted as due to a $(3 \times 2\sqrt{3})$ superlattice. Therefore, this superlattice seemed energetically favoured for all the alkanethiols irrespective of their chain length. Recently, the same system has been investigated by means of low energy electron diffraction (LEED) [23], providing a different interpretation of the diffraction pattern obtained by dosing CH_3S following the same procedure as [22]. In fact, the observed LEED pattern, which was compatible with the reported HAS pattern, was interpreted as due to two distinct coexisting phases, i.e. the $(\sqrt{3} \times \sqrt{3})$ structure and a novel (3×4) phase, rather than to the $(3 \times 2\sqrt{3})$ superlattice. The discrepancy between these results and the previous He scattering data was regarded as due to the low resolution of the HAS apparatus which could not discriminate between the two structures. In order to confirm the LEED results, and to provide new insight into the formation of the CH_3S monolayer, we investigate here the ordered phases obtained by the deposition of DMDS on Au(111) by means of low energy He atom scattering with improved resolution with respect to [22]. In particular, we present an analysis of the diffraction patterns measured at low temperature on films which show the coexistence between the $(\sqrt{3} \times \sqrt{3})$ and the (3×4) periodicity and provide a new protocol for its formation, which does not include re-dosing and annealing cycles. Moreover we present new LEED measurements performed as a function of temperature between 150 and 320 K, showing the occurrence of a $(3 \times 4) - (\sqrt{3} \times \sqrt{3})$ phase transition around 320 K.

2. Experimental method

He atom scattering measurements have been carried out by means of the custom-built scattering apparatus described in detail elsewhere [24, 25] and whose resolution (scattering coherence length) was estimated in [26]. Briefly, the supersonic nozzle beam is produced at source temperature $T_0 = 44$ K. The most probable beam energy is $E = 8.92$ meV, corresponding to an incident scattering wavevector $k_i = 4.13$ Å^{-1}. The scattered atoms are collected by using a time of flight detection system whose axis forms an angle $\theta_t = 110°$ with respect to the incident beam. The incident angle θ_i and the scattering angle θ_f are changed simultaneously by rotating the sample during the angular scans ($\theta_i + \theta_f = \theta_t$). In regions of relatively high intensity, the signal is acquired by a lock-in amplifier to speed up the acquisition. Instead, generally for very weak peaks, the acquired time of flight spectra are integrated around the elastic arrival time and this intensity is used to construct the angular scans. These scans are finally converted

to a parallel momentum exchange scale through the relationship $\Delta K = k_i(\sin(\theta_f) - \sin(\theta_i))$. The measurements have been mainly performed at 150 K in order to maximize the elastic contribution to the scattering. Several polar (θ_i) scans were measured at different azimuthal angles to cover a range of about 40° (which contains the ⟨110⟩ and ⟨112⟩ symmetry directions of the Au(111) surface) in 1° steps to map the reciprocal 2D mesh of the film.

LEED measurements have been performed at beam energies varying between 60 and 110 eV; diffraction patterns have been acquired by a CCD camera, which increases the sensitivity and allows us to minimize the surface exposure to the electron beam. Organic molecules are indeed known to be significantly damaged by electron beam irradiation. For this reason, we maintain an exposure time of few tens of seconds, with a beam current density estimated to be about 50 nA mm^{-2}. In fact, under this current density, we observe in test measurements that the LEED pattern begins to deteriorate after a few minutes; on the basis of this evidence, we assume that for a short exposure the beam damage is a minor problem, though for prolonged measurements it cannot be neglected.

For both experiments, the Au sample is cleaned in ultrahigh vacuum by Ar^+ ion sputtering at 1.5 keV at room temperature followed by an annealing to 750–800 K. For dosing, a stainless steel vial, which contains the purified DMDS, has been directly attached to a leak valve mounted on the target chamber of both experimental set-ups. Before the first dosing, in order to further purify the compound, three freeze–pump–thaw cycles have been performed.

3. Results and discussion

3.1. Phase formation and characterization

Two main different protocols have been tested in order to grow the organic film.

In protocol **1**, the organic film is prepared basically following the procedure of reference [22], by exposing the clean Au surface to DMDS while cooling the sample between 320 and 280 K. We dose into the target chamber at a pressure of 8×10^{-7} mbar for 200 s, which correspond to a dose of about 120 langmuir (1 langmuir = 1×10^{-6} torr). Subsequently the sample is annealed at room temperature (RT) overnight.

In protocol **2** instead DMDS is dosed at constant temperature (304 K) but at a higher pressure of 2×10^{-5} for 120 s, which corresponds to a dose of 2400 langmuir.

In figure 1, typical diffraction patterns measured on the film prepared with **1** are shown. The patterns shown in figure 1(a) have been measured along the ⟨110⟩ direction of the underlying Au(111) surface and the peak at about 1.45 Å^{-1} corresponds to the $(\sqrt{3} \times \sqrt{3})$ periodicity. The peak is well resolved but is weak. By fitting the peaks using Lorentzian functions with a sloping background, a rough estimate of the corresponding domain size can be calculated by the width of the peak, leading to a value of about 130 Å.

In figure 1(b), measurements collected at about 4° off the ⟨110⟩ direction show the presence of other peaks. Two well resolved peaks are detected with an intensity greater than the $\sqrt{3}$ peak. Along the ⟨112⟩ direction, depicted in figure 1(c), the measurements also show an intense peak at about 0.65 Å^{-1} and a small peak at 1.25 Å^{-1}. Performing the same fitting procedure on these other peaks, the corresponding domain size is about 400 Å. In order to confirm that these extra peaks belong to the (3×4) structure, in figure 2 the comparison between the (3×4) mesh and the estimated position of the measured peaks obtained with **1** is shown. Taking into account that six different domains can contribute to the observed diffraction patterns, the reciprocal lattice points belonging to these domains are reported as triangles, while the arrow indicates the position expected for the $(\sqrt{3} \times \sqrt{3})$ periodicity. The experimental peaks are represented by circles. Along the ⟨112⟩ not all the (3×4) spots are detected but the overall agreement between the (3×4) mesh and the experimental data is excellent. The detection of all these

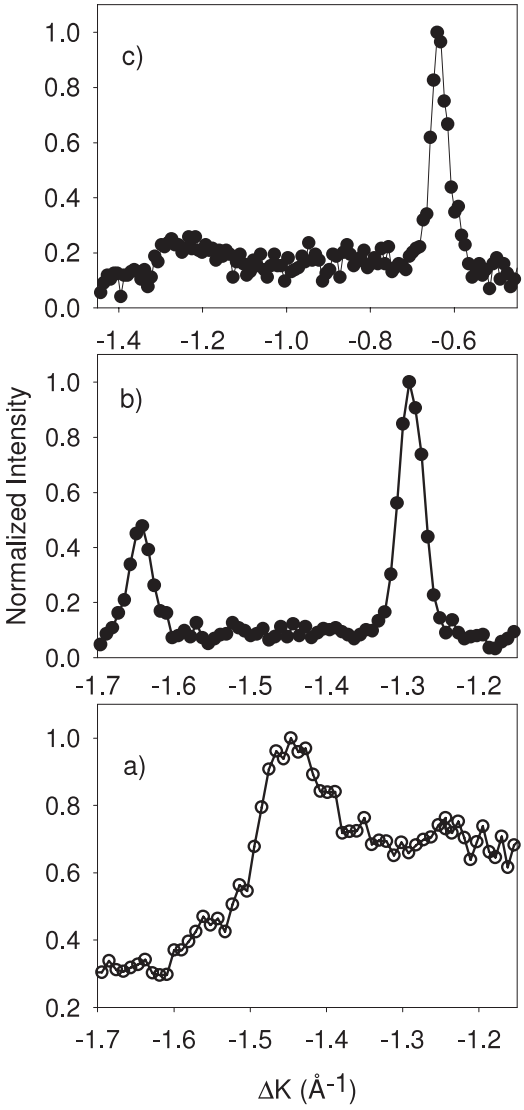

Figure 1. He diffraction patterns measured at 150 K along the ⟨110⟩ direction (a), along a direction 4° off the ⟨110⟩ (b) and along the ⟨112⟩ direction (c). The intensity has been normalized for sake of clarity. Open symbols correspond to measurements performed with the time of flight detection while solid ones are collected by lock-in amplifier. Measurements are taken from a film grown with protocol **1**.

peaks confirms that the structure of the organic film presents the (3×4) periodicity and this coexists with the $(\sqrt{3} \times \sqrt{3})$ one [23]. Instead, the measurements are not consistent with the $(3 \times 2\sqrt{3})$ superlattice proposed in [22] and depicted in figure 2 as squares. Indeed, the two sets of reciprocal lattice points give rise to different features very close to each other. Only with a good angular resolution we have been able to discriminate between the two structures. For instance, near the ⟨110⟩ direction and around the $(\sqrt{3} \times \sqrt{3})$ point, the $(3 \times 2\sqrt{3})$ spots form a triangle not detected in the experiment, while on the contrary the (3×4) spots, located in a hexagonal pattern, are observed (figure 1(b)).

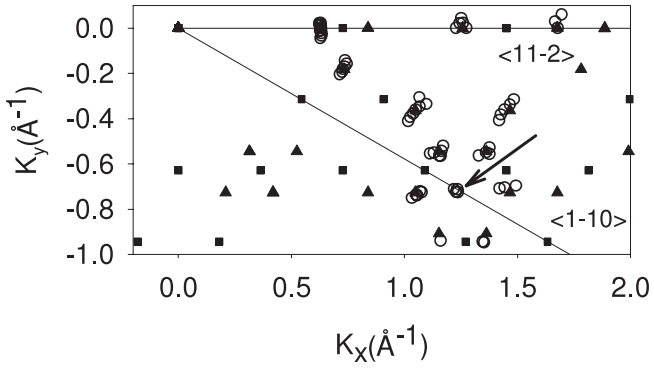

Figure 2. Experimental points (open circles) corresponding to the estimated positions of the diffraction peaks superimposed on the reciprocal lattice of the (3 × 4) structure (triangles). The $(3 \times 2\sqrt{3})$ reciprocal lattice is also drawn for comparison (squares). The two solid lines indicate the Au(111) symmetry directions, ⟨112⟩ and ⟨110⟩ respectively. The arrow points to the position of the $(\sqrt{3} \times \sqrt{3})$ peak at the centre of the hexagonal pattern generated by the (3 × 4) reciprocal lattice points.

In order to explore the stability and reproducibility of the obtained coexisting phases, we modify protocol **1** varying both the deposition temperature and the dose of DMDS. The coexistence of the two phases, though with an intensity and a domain size which depend on the detail of the adopted protocol, is already observed for a dose of 50 langmuir. On the other hand, a low dose seems hampering the formation of well ordered (3 × 4) phase, as shown by the relatively small domain size (about 100 Å). Indeed, a way to improve the (3 × 4) phase quality is provided by further depositions of DMDS before (or during) RT annealing [22, 23]. As these findings suggest that a better (3 × 4) quality can be obtained by substantial dosing, we tried to increase DMDS exposure following protocol **2**. The diffraction patterns measured at 304 K immediately after the deposition are shown in figure 3. The peak associated to the $(\sqrt{3} \times \sqrt{3})$, depicted in figure 3(a), is observed along with the (3 × 4) peak measured in the direction 4° off the ⟨110⟩. By using the same fitting procedure described above, the domain size is 370 Å for the $\sqrt{3}$ phase while is 274 Å for the (3×4) one, showing that the quality of the film obtained by means of **2** is good and, most important, that dosing at high pressure and around 300 K results in the immediate formation of both coexisting phases without any need of further deposition or annealing. Therefore, these results suggest that a dose increase is beneficial to obtain the growth of a (3 × 4); on the other hand, an influence of the deposition pressure on the kinetic of the process ought to be also taken into account. Moreover, as discussed in the following section, the ordering of this system has been found to display a strong temperature dependence. Hence the exposure and annealing temperature could also play a fundamental role in the determination of the degree of order of the film and on the ratio between the two phases. Moreover, as indicated by the observed hysteresis behaviour discussed in the next section and by preliminary HAS measurements performed varying the deposition temperature, the temporal evolution of the film toward equilibrium (particularly concerning the proportion between the amounts of the two phases) can take several hours and is critically dependent on the deposition temperature.

3.2. Temperature dependence

The temperature dependence of the coexisting (3 × 4) phase, prepared following protocol **1**, has been studied by means of LEED. In figure 4(a) selected region of the LEED pattern centred

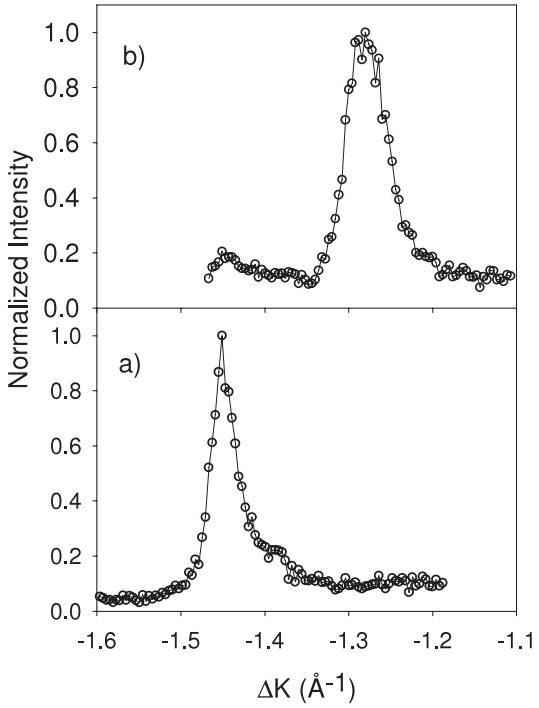

Figure 3. He diffraction peaks measured at 304 K along the ⟨110⟩ direction (a) and along a direction 4° off the ⟨110⟩ (b) from a film grown with protocol **2**. The intensity has been normalized and the measurements have been performed with the time of flight detection.

at the $(\sqrt{3} \times \sqrt{3})$ spot is displayed at different temperatures, clearly showing that around 320 K the (3×4) phase disappears, while the $(\sqrt{3} \times \sqrt{3})$ peak intensity increases.

The low panel in figure 4 shows that upon cooling to low temperature the (3×4) pattern reappear, though not immediately but after several hours. In order to gain more quantitative information on this behaviour, the peak profiles taken across adjacent $(\sqrt{3} \times \sqrt{3})$ and (3×4) spots (see the inset) are shown in figure 5, as a function of temperature in the 110–320 K range for another series of measurements. We note that in this new series, the initial intensity of the $(\sqrt{3} \times \sqrt{3})$ (i.e. the $(1/3, 1/3)$ peak, as indicated in the figure) is quite small, showing that, in agreement with HAS results, the ratio between the two phases is strongly dependent on the preparation conditions. Already at 300 K, the $(1/3, 1/3)$ increases, while the (3×4) peaks at the right side of the spectra strongly decreases. At around 315 K the (3×4) peaks are almost completely disappeared, while $\sqrt{3}$ peak intensity is concomitantly further increasing. Upon lowering the temperature below 320 K the (3×4) peaks almost recover their low temperature intensity only after several hours (one night), as shown by the empty-symbol spectrum in figure 5. The recovery of the (3×4) phase at low temperature indicates that the observed temperature dependence is reversible on the timescale of several hours and rules out the occurrence of desorption processes at high temperature. The somewhat lower intensity of the recovered (3×4) phase relative to the initial one (see figure 5) is indeed ascribable to electron beam damage of the surface caused by prolonged exposure.

The reported temperature and time behaviour clearly indicates that the system undergoes a $(3 \times 4) \rightarrow (\sqrt{3} \times \sqrt{3})$ phase transition at around 315 ± 10 K, in partial agreement with STM/LEED findings reported by Kondoh *et al* [27]. Due to the different symmetries of the two

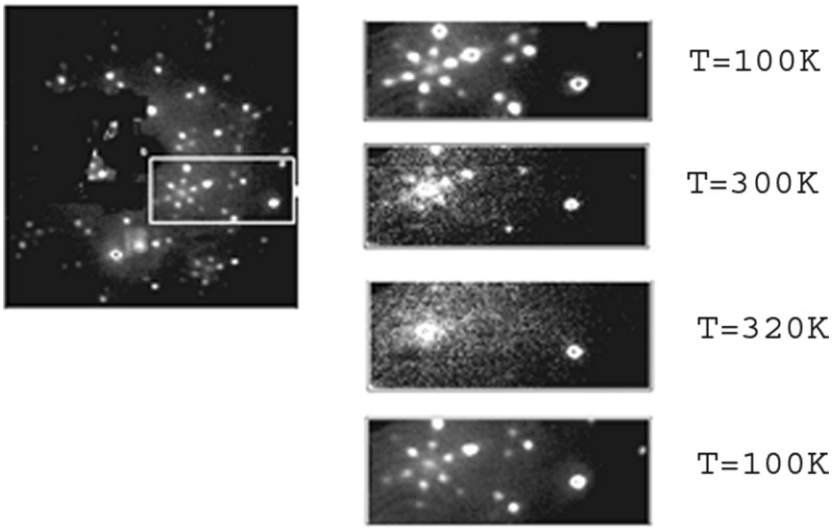

Figure 4. LEED pattern of the coexisting (3×4) phase. On the right the temperature dependence of a zoomed region, where both (3×4) and $(\sqrt{3} \times \sqrt{3})$ peaks are present, is displayed. The low panel represents the LEED pattern taken at 100 K after one-night recovery at RT. The intensity scale is not the same for the different panels and therefore the background intensity increase at around 300 K is only apparent.

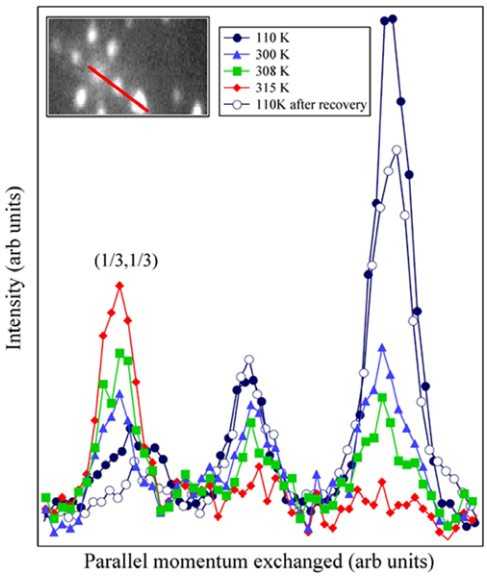

Figure 5. Peak profile taken across the (3×4) and $(\sqrt{3} \times \sqrt{3})$ as a function of temperature. The empty-symbol curve has been taken the following morning and corresponds to the recovered system. In the inset the line across which the profile are taken is shown.

(This figure is in colour only in the electronic version)

structures, the phase transition can be predicted to be of first order. Indeed, this is confirmed by the two following experimental findings, which are fingerprints of a first-order character:

(i) phase coexistence at low temperatures, (ii) the time evolution of the (3×4) recovery, which indicates an hysteresis behaviour, i.e. a 'supercooling effect', with the persistence of the high temperature $(\sqrt{3} \times \sqrt{3})$ phase at temperatures below the phase transition. It is interesting to notice that, according to a very recent work by Mazzarello *et al* [28], the RT structure of the CH_3S/Au(111) $(\sqrt{3} \times \sqrt{3})$ phase at RT is actually obtained by a dynamical equilibrium between the bridge site and a novel motif formed by two CH_3S radicals which are bound to a gold adatom lifted from the gold substrate. According to this work, the interface results quite rough and a certain amount of disorder is therefore expected. The background intensity in the observed LEED pattern could be possibly connected to such disorder, which may be also present at low temperature, due to the coexistence of the two phases. A quantitative estimate of the disorder amount is not easily extracted from our LEED data; it is nevertheless important to mention that the increase in background intensity at around 300 K shown in figure 4 is actually only apparent (see figure 5 for comparison) and is due to the different greyscale used for each picture.

4. Conclusions

We have investigated the structure of the organic film obtained by the deposition of DMDS on Au(111). The techniques employed are He atom scattering at thermal energies, that ensures the absence of any perturbation or damage of the film during the collection of the diffraction intensities, and LEED, that allows a quick and easy determination of the ordered phase symmetry, with the drawback of possible beam-induced damage. The observed He diffraction patterns at 150 K confirm the coexistence of $(\sqrt{3} \times \sqrt{3})$ and (3×4) structures, in agreement with previous and present results obtained by means of LEED [23].

The results contrast the interpretation of a previous He scattering experiment with lower angular resolution, in which a $(\sqrt{3} \times 2\sqrt{3})$ structure was envisaged [22]. Moreover, we have found that a high dose at high pressure (protocol **2**) allows the growth of both phases without any further dosing and annealing. Temperature dependent LEED measurements indicate that the two phases coexist at temperature lower than 320 K, while a phase transition to the $(\sqrt{3} \times \sqrt{3})$ occurs above this temperature. X-ray photoemission measurements (results not shown) performed on the coexisting (3×4) phase obtained by protocol **1** indicate that the fractional coverage of this phase is the same (within the experimental uncertainty) of that of the $(\sqrt{3} \times \sqrt{3})$ phase. The equal molecular coverage of the two phases is also confirmed by the reversible character of the phase transition. In conclusion, this paper clearly shows that even for the simplest among all self-assembled monolayer systems, the determination of the equilibrium structure, which is driven by a subtle balance between different driving forces, is by no means straightforward. In particular, the existence of a first-order phase transition indicates that the entropic factor may play an important role in the determination of the final structure. The dependence of the self-assembled monolayer formation on the kinetic and thermodynamic parameters (i.e. time of exposure, temperature of exposure and of annealing) is currently subject to further investigations.

Acknowledgments

This work was partially supported by the Italian MIUR through Grant PRIN No. 2006020543-003 and through FIRB 'Nanodispositivi Molecolari'. We thank Professor G Scoles and Dr L Casalis for helpful discussions and Mr A Gussoni for technical support.

References

[1] Ulman A 1996 *Chem. Rev.* **96** 1533
[2] Prime K L and Whitesides G M 1991 *Science* **252** 1164
[3] Scherer J, Vogt M R, Magnussen O M and Behm R J 1997 *Langmuir* **13** 7045
[4] Xiao X, Hu J, Charych D H and Salmeron M 1996 *Langmuir* **12** 235
[5] Liu G Y, Xu S and Qian Y L 2000 *Acc. Chem. Res.* **33** 457
[6] Ulman A 1991 *An Introduction to Ultra-thin Organic Films* (New York: Academic)
[7] Schreiber F 2000 *Prog. Surf. Sci.* **65** 151
[8] Alves C A, Smith E L and Porter M D 1992 *J. Am. Chem. Soc.* **114** 1222
[9] Widrig C A, Alves C A and Porter M D 1991 *J. Am. Chem. Soc.* **113** 2805
[10] Fenter P, Eberhardt A and Eisenberger P 1994 *Science* **266** 1216
[11] Fenter P, Eberhardt A, Liang K S and Eisenberger P 1997 *J. Chem. Phys.* **106** 1600
[12] Camillone N III, Leung T Y B and Scoles G 1997 *Surf. Sci.* **373** 333
[13] Schwartz P, Schreiber F, Eisenberger P and Scoles G 1999 *Surf. Sci.* **423** 208
[14] Camillone N III *et al* 1993 *J. Chem. Phys.* **99** 744
[15] Poirier G E and Tarlov M J 1994 *Langmuir* **10** 2853
[16] Delamarche E *et al* 1994 *Langmuir* **10** 2869
[17] Dishner M H, Hemminger J C and Feher F J 1997 *Langmuir* **13** 2318
[18] Nuzzo R G, Zegarski B R and Dubois L H 1987 *J. Am. Chem. Soc.* **109** 733
[19] Ishida T *et al* 1997 *Langmuir* **13** 3262
[20] Heister K *et al* 1999 *Langmuir* **15** 5440
[21] Noh J and Hara M 2000 *Langmuir* **16** 2045
[22] Danisman M F, Casalis L, Bracco G and Scoles G 2002 *J. Phys. Chem.* B **106** 11771
[23] De Renzi V *et al* 2004 *J. Phys. Chem.* B **108** 16
[24] Pedemonte L, Gussoni A, Tatarek R and Bracco G 2002 *Rev. Sci. Instrum.* **73** 4257
[25] Pedemonte L, Tatarek R and Bracco G 2003 *Rev. Sci. Instrum.* **74** 4404
[26] Pedemonte L *et al* 2003 *Phys. Rev.* B **68** 115431
[27] Kondoh H and Nozoye H 1999 *J. Phys. Chem.* B **103** 2585
[28] Mazzarello R, Cossaro A, Verdini A, Rousseau R, Casalis L, Danisman M F, Floreano L, Scandolo S, Morgante A and Scoles G 2007 *Phys. Rev. Lett.* **98** 016102